Delineating Forest Canopy Species in the Northeastern United States Using Multi-Temporal TM Imagery

John G. Mickelson, Jr., Daniel L. Civco, and John A. Silander, Jr.

Abstract

We generated a detailed forest type map of the dominant canopy species within northwestern Connecticut using multi-seasonal Landsat Thematic Mapper (TM) data which were ground referenced with the Global Positioning System (GPS). The map was designed as a calibration layer for a spatially explicit forest dynamics model we have developed, called SORTIE, and will allow us to test the model's effectiveness in predicting landscape level patterns. The precisely located field data were used to derive the forest class signatures used in the classification. Combining the six reflective bands each from spring, summer, and fall Landsat TM images to create an 18-band composite allowed for genus level forest classification precision. We delineated a total of 33 forest classes: 20 dominant types with 13 additional sub-classes representing differing understory composition. Accuracy assessment using the Gopal-Woodcock fuzzy set process returned an overall forest class accuracy of 78.9 percent at the procedure's Acceptable *level.*

Introduction

The field of remote sensing has added greatly to our ability to understand forested systems, with the production of increasingly detailed maps and attribute sets, from the level of the stand to the landscape. Surprisingly, few studies have been published which document efforts to use satellite data to map the mixed deciduous temperate forest types of the northeastern United States at Anderson Level 2 or better (Anderson *et al.*, 1976). The many broad scale efforts undertaken (Brown *et al.*, 1993; Goward *et al.*, 1985; Loveland *et al.*, 1991; Townshend *et al.*, 1991; Zhu and Evans, 1994) have delivered regionally generalized cover types with thematic and spatial resolutions too broad to assist adequately local forest researchers and resource managers focusing on smaller scales. The few remote sensing studies analyzing forested systems of the Northeast (Bryant *et al.*, 1980; Herwitz *et al.*, 1990; Nelson *et al.*, 1984; Rock and Vogelmann, 1989; Vogelmann, 1988; Vogelmann and Rock, 1989) have effectively omitted attempts to delineate among deciduous forest types.

Acceptable estimates of detailed forest cover for New England and the compositionally similar Great Lakes States are now being obtained by researchers using multi-seasonal remotely sensed imagery. Using phenological change information in a layered approach, Wolter *et al.* (1995) have recently mapped forest classes in northern Wisconsin at the genus and species level, where previously only generalized Anderson Level 2 (coniferous/deciduous/mixed) delineation was achieved (Bauer *et al.*, 1994; Beaubien, 1979; Benson and DeGloria, 1985; Karteris, 1990). Slaymaker *et al.* (1995) obtained class detail for the forests within New England at Anderson Levels 3 and 4, with a total of 30 forest classes, using GPS-referenced videography to interpret a summer/fall clustered TM image sequence.

Vast and rapid improvements in technological capabilities have no doubt facilitated much of this progress. Access to faster and more capable computer platforms has aided our ability to store and process larger and more detailed image and attribute sets. The Global Positioning System (GPS) has provided a precise and cost-effective ground referencing method to aid in relating the information from multi-temporal and multi-source digital data layers to the patterns and processes recorded within field plots. These advances have allowed us to extend the scope of our analysis of the spatial, spectral, and contextual patterns within natural systems across more complete four-dimensional fields; *X*, *Y*, *Z* (elevation), and *T* (time). We can, in effect, more effectively recognize and incorporate patterns from a wider array of source data. For instance, Lee *et al.* (1989), Franklin and Peddle (1989), and Woodcock *et al.* (1994) have shown that adding spatial or spectral texture information for coniferous and mixed forest types can significantly improve map classification accuracy. Linking biogeographic data with knowledge of specific species response patterns to variables such as soils, elevation, slope, and aspect has evolved as a commonly accepted method for improving vegetation maps in many areas (Damman and Kershner, 1977; Damman, 1979; Bolstad and Lillesand, 1992; Lee *et al.*, 1992; Brown *et al.*, 1993; Goodchild, 1994). Tracking differences in spectral reflectance at the landscape scale level with multi-date imagery allows us to detect the apparent change of cover type at a specific geographical location, for example, deforestation (Varjo, 1996) or the emergence and senescence of a wheat field (Reed *et al.*, 1994).

The overall purpose of our study was to develop a detailed forest-cover type map as a calibration layer for a forest dynamics model we have developed, named SORTIE. SORTIE is a spatially explicit explanatory and predictive forest dynamics model that was calibrated from field data to approxi-

J.G. Mickelson and D.L. Civco are with the Department of Natural Resources Management & Engineering, University of Connecticut, Storrs, CT 06269 (jmickel@canrl.cag.uconn.edu; dcivco@canrl.cag.uconn.edu).

J.A. Silander is with the Department of Ecology and Evolutionary Biology, University of Connecticut, Storrs, CT 06269 (silander@uconnvm.uconn.edu).

Photogrammetric Engineering & Remote Sensing, Vol. 64, No. 9, September 1998, pp. 891–904.

0099-1112/98/6409–891$3.00/0
© 1998 American Society for Photogrammetry and Remote Sensing

American Society of Photogrammetry and Remote Sensing: ERDAS Award paper, 1999

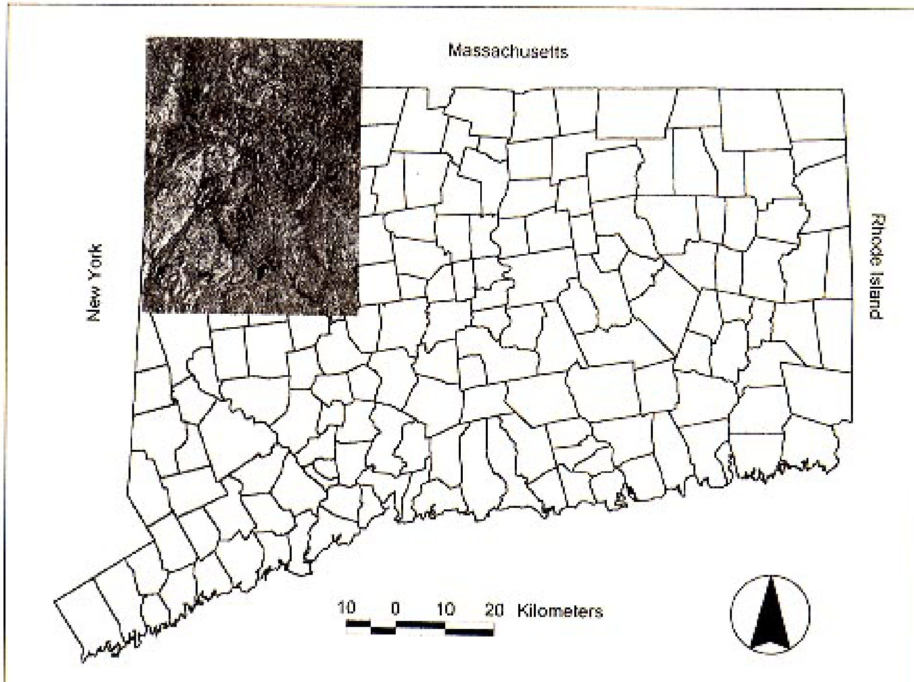

Figure 1. Study site location. 04 May 1988. TM Band 5.

mate stand level interactions of individual trees. It was constructed from four sub-models that estimate performance parameters for propagule dispersal, recruitment, growth, and mortality as well as functions of local resource availability, primarily light (Pacala *et al.*, 1993). Accurate predictions of the dynamics and species compositions of stands have been produced (Pacala *et al.*, 1996) for intermediate soil moisture and nutrient conditions.

Among our project goals was the production of an independent test of a landscape version of SORTIE. For this purpose, a map depicting the region's ten dominant canopy trees and forest types was generated to test the model at varying scales and levels of complexity. Because we wished to study apparent vegetation gradient relationships derived from overlays of our output map with ancillary digital layers (soils, elevation, slope, aspect) and compare them with SORTIE outputs, biogeographic data were not utilized to aid this portion of the classification. Only the spectral patterns from the TM data were considered in order to avoid circularity in the classification and subsequent overlay process. The results from the forest type map and biogeographic data overlays are reported elsewhere (Mickelson, 1997). The objective of this project was to assess whether the spectral patterns contained within multi-seasonal TM data could be used to improve discrimination among the forest canopy species in northwestern Connecticut. This paper describes the utilization of multi-seasonal TM data and GPS-referenced ground data to produce a forest type map at Anderson Levels 3 and 4.

Methods

Study Site

The study site comprises 16 USGS 7½-minute quadrangles in the northwestern highlands of Connecticut, an area of approximately 240,000 hectares (Figure 1). The dominant forest-cover types have been described as transitional between oak-hickory central hardwood and northern hardwood forest associations (Eyre, 1980). Soils are predominantly inceptisols with occasional spodsolic areas and span from rich moist calcareous bottomlands to dry, thin nutrient poor ridges. Relief ranges from 150 to 550 metres above sea level. The underlying geological formations are highly metamorphosed Precambrian gneisses and shists with inclusions of limestone and marble. Glacial till and glacio-fluvial deposits overlie most of the bedrock. Rainfall averages 1220 mm per year and is evenly distributed throughout the year.

The U. S. Forest Service (Dickson and McAfee, 1985) lists the ten dominant species for Litchfield county, in relative abundance, as red oak (*Quercus rubra L.*), red maple (*Acer rubrum L.*), hemlock (*Tsuga canadensis L.*), white pine (*Pinus strobus L.*), American beech (*Fagus grandifolia Ehrh.*), sugar maple (*Acer saccharum Marsh.*), white ash (*Fraxinus americana L.*), yellow birch (*Betula alleghenіensis Britt.*), white oak (*Quercus alba L.*), and black cherry (*Prunus serotina Ehrh.*). These are also the species for which SORTIE was calibrated. Common understory associates which we found to affect spectral responses include mountain laurel (*Kalmia latifolia L.*) and juvenile hemlock. Intensive land-use practices over the past 300 years (Egler, 1940; Winer, 1955; Westveldt *et al.*, 1956; Foster, 1992) include charcoaling of hardwoods and intensive softwood harvesting, with most of the landscape having been cleared and allowed to regenerate repeatedly. Such widespread impacts have helped lead to the great compositional and structural heterogeneity of today's forest (Foster, 1993).

GPS Field Sampling

Field sampling was conducted according to a modified Damman method (Damman and Kershner, 1977), with all sites being sampled prior to image classification. The purpose was to provide a detailed characterization of the composition and structure of each sample plot (SP) on a per-pixel basis for canopy and understory, and to relate those features to the corresponding spectral patterns within the layered TM image. The percent composition (total of 100 percent) for each canopy species greater than 10 cm in diameter was visually estimated for a 30-m radius at 405 SPs. Additional estimates were taken for the type and percent composition of understory (2 to 5

TABLE 1. KMEANS CLUSTER/CLASS-SUBCLASS DESCRIPTORS

1. *RO*
Red oak dominated stands
Mean 83% min. 70% with other hardwoods minor components.
 2. *RO/LU* – as above with mt. laurel understory
3. *RO/Mx*
Red oak stands with mixed hardwoods.
Red oak mean 55%, min. 35% with mixed hardwoods.
 4. *RO/MX/LU* – as above with mt. laurel understory
 5. *RO/MX/HU* – as above with hemlock understory
6. *OAK/Mx*
White oak dominated stands
Mean 40% min. 20% with chestnut oak, red oak, red maple.
 7. *OAK/Mx/LU* – as above with mt. laurel understory
8. *RO/RM*
Mixed red oak and red maple stands.
Red oak mean 33% min. 15% min., red maple mean 29% min. 15% with mixed hardwood.
 9. *RO/RM/LU* – as above with mt. laurel understory
 10. *RO/RM/HU* – as above with hemlock understory
11. *RM*
Red maple dominated stands
Mean 63% min. 45% with mixed hardwoods
 12. *RM/HU* – as above with hemlock understory
 13. *RM/LU* – as above with mt. laurel understory
14. *SM*
Sugar maple dominated stands
Mean 56% min. 38% with white ash.
 15. *SM/HU* – as above with hemlock understory
16. *SM/RO/Mx*
Mixed sugar maple red oak stands
Sugar maple mean 36% min. 20%, red oak mean 36% min. 20% with white Ash and mixed hardwoods.
No subclass
17. *WA/RM/Mx*
Mixed white Ash and red maple stands
White Ash mean 43% min. 20%, with red maple common and mixed hardwoods
18. *WA/RM/WP/Mx* – as above with white pine
19. *BC/SM/Mx*
Black Cherry with sugar maple stands with mixed hardwoods
Cherry mean 42% min. 25%, sugar maple mean 37% min. 15%. White ash common.
No Subclass
20. *Be*
Beech dominated stands
Beech mean 67% min. 50% with sugar maple, red oak, and hemlock
 21. *Be/Hu* – as above with hemlock understory
22. *NHd/Be/SM*
Northern hardwood stands dominated by beech
Beech mean 35% min. 17% with red maple, sugar maple, yellow birch.
 23. *NHd/Be/SM/HU* – as above with hemlock understory
24. *NHd/YB/RM/He*
Mixed northern hardwood/coniferous stands
Dominated by yellow birch, mean 30% min. 10% with red maple and hemlock
No Subclass
25. *MxHd*
Mixed hardwood no specific dominance.
Mostly red oak, white ash, red maple, sugar maple, mixed birches.
 26. *MxHd/HU* – as above with hemlock understory
27. *Mx/Hd/WP*
Mixed hardwood/white pine stands
Dominated by black cherry mean 53% min. 35%, with white pine and red maple.
No Subclass
28. *WP*
White pine dominated stands
White pine mean 85% min. 50%, with white ash, red maple, red oak
No Subclass
29. *P/MxConif*
Red pine dominated stands
Red pine mean 90% min. 85%, white pine, hemlock, spruce, and mixed conifers common.
No Subclasses
30. *He/RM*
Hemlock and red maple dominated. stands.
Hemlock, mean 38% min. 16%, red maple mean 38% with hardwoods.
No Subclass
31. *He/MxHd*
Mixed hemlock and hardwood stands
Hemlock mean 49% min. 30% with red maple, red oak, mixed hardwoods.
No Subclass
32. *He*
Hemlock dominated stands
Mean 80% min. 65% with red maple, Beech, Yellow Birch.
No Subclass
33. *Sp*
Black or red spruce dominated stands
Mean 91% min. 85%. With minor components of hemlock and red maple.
No Subclasses

metres in height) and herb layer (1 to 2 metres) for the evergreen species, hemlock and mountain laurel. Hemlock understory (HU) and laurel understory (LU) indices were calculated by multiplying the total percent cover of the understory and herb layer by the percent composition accounted for by either species. Index values ranged from 0 to 25, with 0 representing a site with no sub-canopy component to 25 for a site completely covered by a combination of either species. All sites were within three miles of a road in order to reduce travel time between SPs. Three-hundred and ten of the plots were selected to be at least 150 meters from a boundary with a differing composition or structure type. This was done to maintain accurate site depictions, once GPS and satellite pixel misregistration (optimally, 2 to 5 metres and 15 metres, respectively) were taken into account. We received data for another 95 plots, which were acquired in a random manner, with plots falling within a compositional gradient between cover types. Universal Transverse Mercator eastings and northings for each plot were determined by averaging 180 differentially corrected GPS point readings. Field checks on Connecticut geodetic survey monument markers showed the GPS accuracy to be within 2 to 5 metres.

Forest Cover-Type Class Generation

We wished to develop and test a reproducible vegetation classification procedure, which would be constructed from the TM spectral data alone. Existing classifications, which are based on vegetation or taxonomic units alone, may not have possessed a sufficiently unique spectral signal to allow for adequate class separability (Treitz *et al.*, 1992; Schreiver and Congalton, 1995). For this reason, we started by classifying the 405 SPs using a K-Means clustering process to produce 20 forest type clusters. Each of these 20 classes was sub-classified based on percent composition of hemlock or mountain laurel in the understory, yielding an additional 13 classes (Tables 1 and 2). Output statistics for the clustered classes reported minimum and mean percent composition for the ten dominant canopy species as well as the understory component. To avoid obvious confusion, none of the 20 dominant classes that contained more than 10 to 15 percent hemlock

Table 2. Percent Species Composition for the Final 33 Forest Cover Types. Initial Grouping of Species Included: *Oak*, all oaks; *RM*, red maple; *SM*, sugar maple; *WA*, white ash; *BC*, black cherry; *Be*, American beech; *Brch*, all birches; *WPm*, white pine; *He*, eastern hemlock; *Sp*, all spruce; *Oth*, other genera; *HU*, hemlock understory index; *LU*, mountain laurel understory index.

Class Number	Forest Class	Class Spp. Composition (%) Total 100												
		Oak	RM	SM	WA	BC	Be	Brch	WPm	He	Sp	Oth	HU	LU
1	*RO*	89	3	2	1	1	1	3	0	0	0	0	0	0
2	*RO/LU*	89	9	0	0	0	0	2	0	0	0	0	0	18
3	*RO/Mx*	73	4	1	4	4	8	2	0	1	0	3	0	1
4	*RO/MX/HU*	53	5	7	1	0	11	4	0	19	0	0	15	0
5	*RO/MX/LU*	72	7	2	0	0	2	8	4	4	0	1	2	17
6	*OAK/Mx*	88	7	1	0	2	0	2	0	0	0	0	2	0
7	*OAK/Mx/LU*	79	10	0	4	0	0	7	0	0	0	0	0	20
8	*RO/RM*	44	28	1	6	3	5	4	1	5	0	3	1	1
9	*RO/RM/HU*	30	27	0	10	1	4	17	1	9	0	1	17	4
10	*RO/RM/LU*	65	33	0	0	0	2	0	0	0	0	0	0	22
11	*RM*	11	61	1	5	8	5	6	1	2	0	0	0	0
12	*RM/HU*	2	63	0	0	0	7	5	13	7	0	3	13	3
13	*RM/LU*	1	69	7	0	4	0	10	4	3	0	2	1	16
14	*SM*	7	5	61	17	4	2	1	0	1	0	2	1	0
15	*SM/HU*	10	10	40	30	0	0	0	0	10	0	0	9	9
16	*SM/RO/Mx*	43	0	36	6	4	3	4	0	2	0	2	1	0
17	*WA/RM/Mx*	11	16	6	49	4	3	7	1	2	0	1	2	1
18	*WA/RM/WP/Mx*	8	14	5	27	2	0	1	37	6	0	0	5	1
19	*BC/MS/Mx*	1	0	37	14	42	0	2	4	0	0	0	1	2
20	*Be*	5	7	3	0	7	68	4	0	6	0	0	1	0
21	*Be/HU*	3	8	5	1	7	67	5	0	4	0	0	13	2
22	*NHd/Be/SM*	7	13	14	3	11	35	6	0	6	0	5	0	0
23	*NHd/Be/SM/HU*	2	25	0	3	7	33	20	0	10	0	0	16	0
24	*NHd/YB/RM/He*	6	22	3	1	10	2	33	3	17	0	3	3	8
25	*MxHd*	37	9	4	13	2	3	17	2	2	0	11	0	0
26	*MxHd/HU*	27	14	4	9	9	3	16	12	4	0	2	6	6
27	*Mx/Hd/WP*	4	11	8	3	42	0	6	26	0	0	0	6	2
28	*WP*	3	4	1	3	1	0	1	85	2	0	0	6	4
29	*P/MxConif*	0	0	0	0	0	0	2	93	5	0	0	8	0
30	*He/RM*	16	11	4	1	3	6	6	2	49	0	1	5	2
31	*He/MxHd*	3	37	2	1	2	5	7	0	39	0	4	0	1
32	*He*	2	6	0	0	1	5	4	1	81	0	0	6	1
33	*Sp*	0	3	0	0	0	0	2	0	3	92	0	8	6

in the canopy were stratified by the evergreen understory. The results of our classification would later be compared to currently used forest cover types (Eyre, 1980).

Remote Sensing

Remote sensing studies of forested systems in the northeastern United States which have focused on pattern extraction from within single date imagery have mostly failed to provide detailed depictions of forested landcover, especially of deciduous types. (Franklin *et al.*, 1986; Moore and Bauer, 1990; Spanner *et al.*, 1990; Bauer *et al.*, 1994). Schreiver and Congalton (1993) showed that deciduous forest type map accuracy for the Northeast can be improved by including multi-seasonal satellite data in the classification procedure. They utilized the seasonally unique spectral patterns of nine southern New Hampshire forest types to delineate among them using spring, late summer, and early fall images. They concluded that the stand differences in foliar presentation and dieback contained within fall and spring images made these data superior to those acquired during the full leaf-out conditions of summer. However, their research focused on classification processes applied to and compared between images of individual seasons, without following patterns that the species might exhibit throughout the year. Slaymaker *et al.* (1995) have incorporated a spring-summer hyperclustered image (12 bands/240 classes) coupled with terrain and neighborhood information to provide detailed forest-type maps of southern New England which include seven Anderson Level 3 forest types and 33 Level 4 subclasses. Our approach is similar to this, though we chose to concatenate the six reflective bands each from three seasonal TM images. This would allow us to test whether analyzing the phenologically dependent spectral patterns extending across an entire growing season would significantly improve species discrimination.

TM Satellite Data Selection

Three Landsat-5 Thematic Mapper images (Path 13/Row 31) were chosen that span seasonal and apparent phenological changes in the forest. These include images for spring (4 May 1988), summer (30 August 1990), and fall (6 October 1992). The images were acquired as precision corrected data from EOSAT, and the May and October scenes were cloud-free. The August scene had less than one percent cloud cover, and we accounted for clouds and their shadows as a combined spectrally classified map unit. The May image captured early budbreak and pre-leafout conditions for most angiosperms in southern New England (Egler, personal communication, 1994) and was chosen to aid in the discrimination of upland deciduous, coniferous, and wetland forests and moist soil conditions. The August scene was used as a baseline summer vegetation layer depicting full leaf-on conditions. The October image was chosen because of its depiction of heightened color and senescent leaf condition for maples and oaks (Smith, 1992). Though the four-year interval between image dates would likely create a change class, we considered the likelihood that this cover type would account for more than a small fraction of the forested scene to be negligible. Thirty road intersections from within the study area were located within both the reference and test imagery, and then referenced on the ground with GPS, to check intra-image spatial registration. Additional inspection

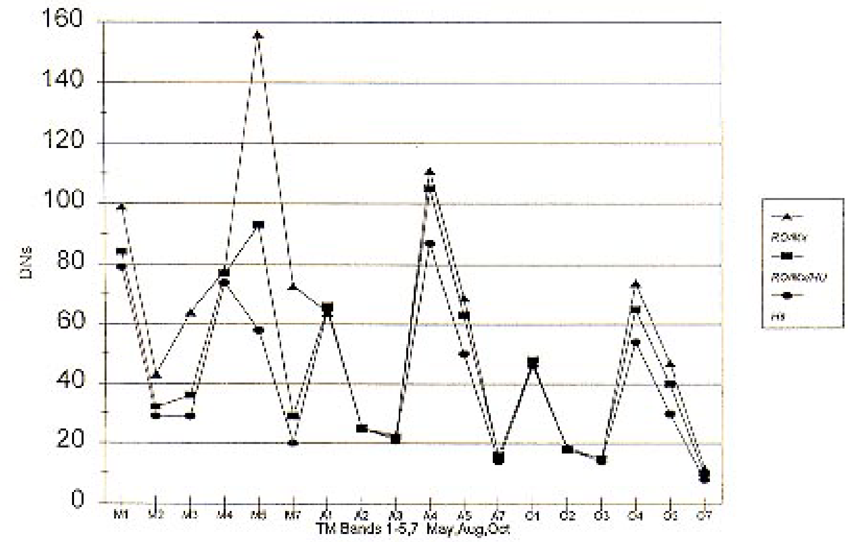

Figure 2. DN values for three sample plots for May, August, October images. *RO/Mx*, a mixed oak/hardwood stand, its clustered hemlock understory subclass *RO/Mx/HU*, and a hemlock dominated stand *He*.

for the presence of "ghosting" along the boundaries of permanent water bodies confirmed the imagery to be approaching the 15-metre (0.5 pixels) RMS error of the data.

Ancillary reference data included region-wide USGS Digital Line Graph (DLG) road and hydrography coverages. These were used to check inter-image registration and alignment of linear features. A SPOT panchromatic image (10-m resolution) from May 1988 was used to verify selection of non-forest class cover type signatures, as were black-and-white 1:12,000-scale aerial photographs from May 1990.

Signature Selection and Image Classification

Initial exploration of our image data suggested that phenological sequences might be used to separate understory subclasses of the dominant canopy types. Figure 2 contains the mean reflectance values across the three image dates for three forest plots: *RO/Mx*, a mixed oak/hardwood stand; its clustered hemlock understory sub-class *RO/Mx/HU*; and a hemlock dominated stand *He*. The stands are clearly stratified within the spectra of the May image, especially within the red and mid-infrared portions of the spectrum (Bands 3, 5, and 7). The hardwood stand exhibits a heightened overall reflectance which is especially demonstated in the red and middle infrared, possibly from the early stages of leaf flush from the juvenile shrub/sub-canopy layer or, more likely, the high reflectance of dried leaf litter on the forest floor (Ripple, 1986; Curran *et al.*, 1991) showing through the canopy. Because, within this scene, components of the oak canopy are exhibiting little leaf-out, the *RO/Mx/HU* stand displays a signature more like the *He* than the mixed oak, because it is principally the hemlock which the sensor detects. As the leaf canopy has fully flushed by the acquisition time of the summer image, the oak masks the hemlock subcanopy, and that same stand most closely matches the spectral pattern of the compositionally similar *RO/Mx* . The October TM image stratifies the classes somewhat further, with the *RO/Mx* class exhibiting a heightened reflectance in the near and middle infrared bands, without the dampening effect of the evergreen components. Classifications run on any single image would likely have sorted the classes differently, likely partitioning the *RO/Mx/HU* as a hemlock stand in the spring scene, as hardwood in the summer, and mixed hardwood/conifer in the fall. We chose to include three seasons in our test data, because signatures exhibited across an entire growing season (18 bands) might provide a unique spectral pattern that would not be found in any single image.

For our classification regime, we adopted a modified traditional hybrid unsupervised-supervised pixel-based classification method (Richards, 1986). Typically during a supervised classification, cover-type signatures are chosen by deriving the mean pixel values from within a user-selected region. These regions are generated in one of two ways. In the first, areas of known or assumed composition are located within a reference data source, such as a forest stand map or aerial photograph. These areas are then located within the digital imagery, and boundaries are drawn around an area of interest (AOI), with the spectral properties (mean vector, variance-covariance, etc.) being calculated from all pixels within the polygon. In the second method, the signature relating to a single specific seed pixel is chosen from within an AOI, and the signatures of contiguous pixels are compared and included, until a preset spatial or spectral threshold is met.

Following the second method, our forest class signatures were region grown within the 18-layered image, but we used the GPS-referenced sample points as the seed pixels. This allowed us to tie the means of the spectral signatures to the detailed species composition that we measured within the precisely located sample plots. To minimize edge effects, a typical spectrally grown region was limited to 8 to 15 pixels (0.72 to 1.35 ha) and was spatially constrained to be contained fully within a larger region of known composition, based on our ground survey. From the 405 sample points, one to three replicates for each of the 33 forest classes (total of 83 SPs) were selected as signatures. Within-class replicates were selected to account for compositional variance as well as a range of site conditions. Ideally, we would have liked to have had a greater number of test plots from which to select both calibration areas as well as test sites for the final classification. Congalton (1991) recommends that an appropriate rule of thumb is to collect 50 samples for each map unit or cover type being derived. However, given the limited time and resources that most projects and ours operate under

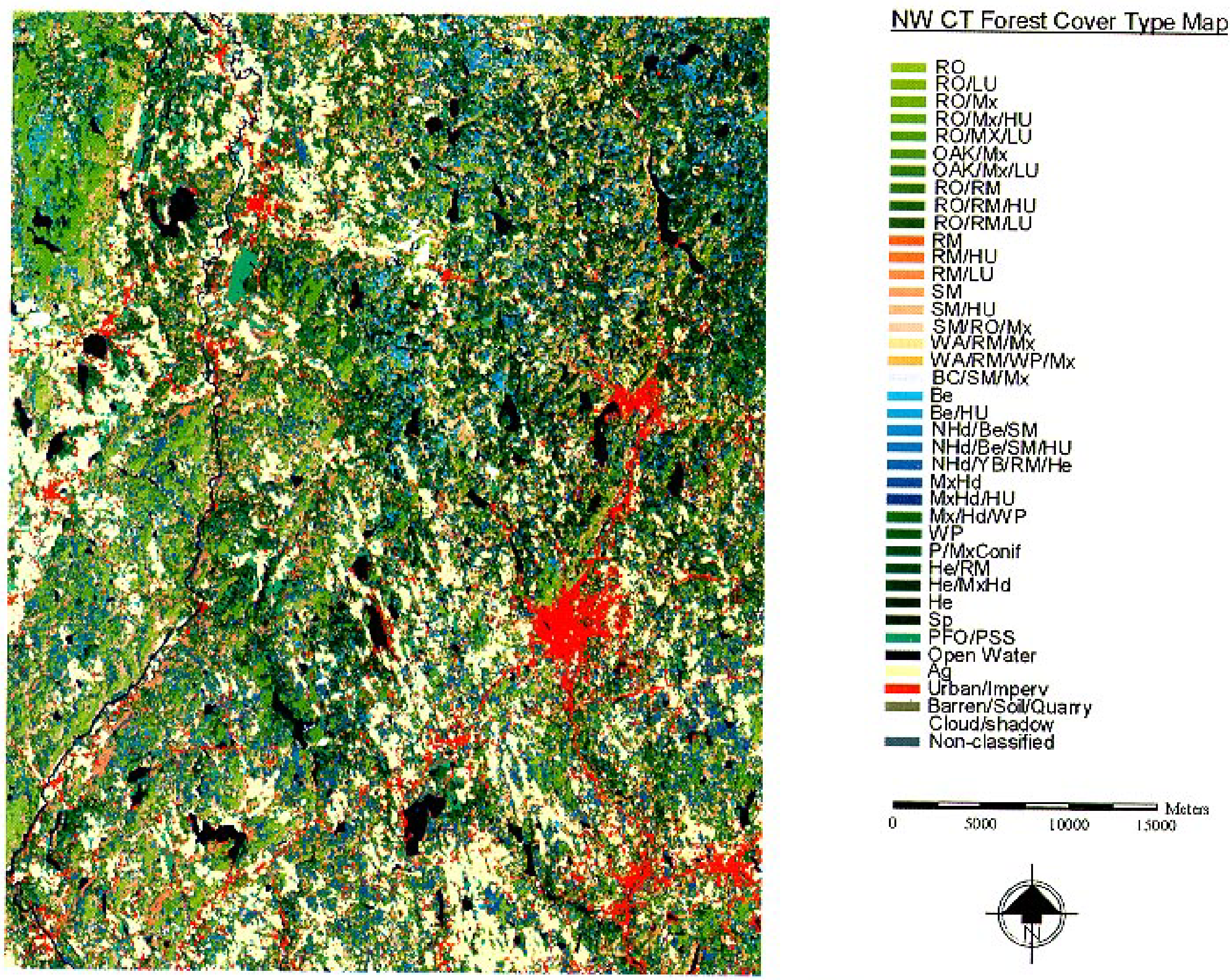

Plate 1. Final 40-class land cover/forest classification.

(Thompson *et al.*, 1996), we felt that the high quality (compositional and spatial accuracy) of our plots compensated for the statistical question of sampling numbers.

Signatures for seven non-forested classes — *open water, urban, agricultural lands, barren, non-forested wetlands, clouds and cloud shadow,* and *unclassified* — were visually selected from a 250 class ISODATA unsupervised classification of the 18-band image. The *unclassified* group contained those pixels within the image which we knew to be commonly confused with one another (coniferous forest, coniferous wetlands, impervious surfaces, shadowed west and northwest facing slopes) (Franklin *et al.*, 1986) and where such a confusion would lead to extreme errors. The unclassified portion of the image represented less than 1.5 percent of the final output map, and will be the subject of future classification refinements. Shadow and topographic influences on the data's radiometric properties were not accounted for in this phase of the analysis in order to retain the imagery's original spectral integrity. Non-forest-class masking was also forgone, due to minor pixel shift effects observed in early masking attempts. The final signatures were checked for confusion within an error matrix, using a minimum-distance metric, with all test signatures achieving less than 25 percent omission rates.

A minimum-distance-to-means classifier (MDM) has been shown to produce accuracy results equal to or exceeding a maximumlikelihood (ML) decision rule in a number of land-cover and forest mapping efforts (Hixon *et al.*, 1980; Thomasson *et al.*, 1994; Zeff and Merry, 1993; Zhuang *et al.*, 1995). This is especially true when the multispectral data are not normally distributed across the information classes. In our own study, preliminary results comparing the two classifiers indicated that MDM also produced an image with less spatial heterogeneity (*salt-and-pepper*) at a fine scale. Third, because the MDM decision rule has less rigorous statistical requirements, because no covariance matrix is required, the region grown around the GCP could be confined to a more spatially discrete area (i.e., contain fewer pixels) than that which the ML rule demands. This allowed for a more precise signature characterization. For these reasons, we utilized an MDM classifier to generate our final classification (Plate 1).

Fuzzy Accuracy Assessment (FAA)

Forest-cover mapping strategies must be sensitive to the specific patterns which the vegetation for a particular locale exhibit (Beaubien, 1979; Damman, 1979; Woodcock and Strahler, 1987). Within the compositionally mixed forests of southern New England, distinct stand boundaries seldom exist. This makes the traditionally difficult decision of where to place class transition lines even more challenging. Even the few species that exhibit clear canopy dominance and form "pure," locally dense stands, e.g., oaks on ridges, red maples in swamps, and hemlocks and white pine in mature stands, follow near continuous gradations from one type into another. This produces great compositional variability at the stand level and spectral overlap (mixed pixels) at the pixel level, and commonly results in moderate map class uncertainty (Wang and Civco, 1992; Manyara and Lein, 1994). A simple binary accuracy assessment procedure (i.e., right versus wrong) seemed inappropriate for assessing the set membership and subsequent forest class boundaries in our study, given the depth of thematic and spatial detail likely to exist in our classified map.

We believe that membership criteria in forest classes for sites such as ours are best dealt with by allowing for multiple set memberships. Fuzzy set theory (Zadeh, 1965; Banyikawa *et al.*, 1990; Wang, 1990; Manyara and Lein, 1994; Woodcock and Gopal, 1992; Woodcock and Gopal, 1992; Woodcock *et al.*, 1994) has been shown to aid in the application of remotely sensed data products by analyzing and quantifying vague, indistinct, or overlapping class memberships. Wang (1990) concluded that much of the information from within digital data can be lost during the course of traditional one-pixel-one-class classification methods, due to efforts to apply "hardened" or discrete classes to mixed pixels containing multiple cover types. Compared to traditional accuracy assessment procedures, the Gopal-Woodcock fuzzy accuracy assessment operator provides useful and otherwise lost information as to the magnitude and frequency of errors, and reports on the distribution of intraclass confusion (Gopal and Woodcock, 1994). For these reasons, a fuzzy accuracy assessment (FAA) program developed at Boston University was employed to evaluate the mapping results (Collins, 1994).

Following the supervised MDM classification procedure, the pixels containing the remaining 322 (405 minus 83) ground sample units were located within the image, and the forest class assigned to those locations was recorded. As input into the FAA program, our 322 test SPs were arranged in a 33-column (Class) by 322-row (SP) matrix. An expert evaluation was calculated for each SP, which grades the degree of acceptability at each site for each of the 33 possible forest classes. The evaluation scale ranged from 5, for best fit, to 1, for poorest fit, as described in Table 3. Genus level interclass error among oaks (red, white, other), maples (red, sugar) and birches (black, yellow, paper, other) were counted as *Acceptable* as were errors where hemlock in the canopy was misclassified as hemlock in the understory. It is at the stage of acceptability rating that the greatest degree of subjectivity is introduced in a fuzzy accuracy assessment. To counter this, we used the simple percent mean cluster similarity index (Ludwig and Reynolds, 1988) to provide an initial quantitative measure of fuzzy ranking. The percent similarity between two classes was calculated as the sum of the minimum percent composition for all species that the two classes had in common; i.e.,

$$\Sigma \min (A_{ij}; A_{ik})$$

where A_{ij} and A_{ik} are the abundances (in percent composition) of all species i in samples j and k. The total percent similarity which was possible between two classes was 125, which included values for the canopy (maximum of 100 percent) as well as the understory index (maximum of 25 percent). Although the threshold criteria were different for many classes, only one *Best* fuzzy rank value of 5 was allowed per class, that of the seed class.

The FAA program successively evaluates the impact on the map's accuracy that classifying each of the test sites *as* each of the possible land-cover classes would have, and outputs the results in three tables. The MAX/RIGHT operator (Table 4) delivers a general measure of the overall accuracy of the map and presents the number and frequency of the ranked errors. It lists the number of test sites which ranked the MAX (5 or *Best*) and those whose sites were ranked as RIGHT (3 or *Acceptable*). The DIFFERENCE metric (Table 5) for a particular test site represents the expert score for that class minus the score for any other higher ranked class. The maximum value possible (5 minus 1) is a score of 4, indicating a class which is perfectly unique (no other classes fit at all) as well as correctly classified. In our case, it is an approximate measure of the amount of overlap, or uniqueness, for a class as well as a value for the magnitude of the map's errors.

TABLE 3. FUZZY ACCURACY ASSESSMENT–EXPERT EVALUATION RANKING SYSTEM.

Fuzzy Score	Ranking	Description
5	Best Possible	Classified as exact class/cluster
4	Very Good	Classified as class, subclass replicate or other with percent cluster similarity typically > 80–85%
3	Acceptable	Classified as other. Genus level interclass discrimination was accepted, e.g. red oak for white oak, red maple for sugar maple, hemlock subdominant canopy for hemlock understory. Similarity typically > 70%.
2	Understandable, but wrong	Usually correct at Anderson Level II (e.g. Coniferous, Deciduous forest), but contains serious problems at genus level of detail. Similarity < 70%
1	Entirely wrong	Absolutely wrong.

Traditional confusion or classification error matrices provide a means of evaluating the thematic accuracy of a classified image, by comparing the class assigned to a group of test pixels to the actual ground information at those sites. The analyst can benefit by identifying which categories are being confused with each other, either by being erroneously excluded from one class (omission error), or included in another (commission error), and determine the seriousness of such an error. In an FAA procedure, the CONFUSION/AMBIGUITY operator provides similar though slightly different information, because multiple classes can be acceptable for any given sample plot (Woodcock *et al.*, 1992), with the number of errors presented actually exceeding the number of test pixels. In addition, values are provided for two levels of error. The CONFUSION value contains the number of instances another map category scored higher than a particular map class. The AMBIGUITY value contains the number of classes whose scores equaled the value for that map category. As in a traditional error matrix, column totals represent errors of omission and the row totals indicate the total commission errors.

Results and Discussion

Overall forest class accuracy was surprisingly good, 78.9 percent at the *Acceptable* or RIGHT level, but rather low, 13 percent, for the MAX level (Table 4). Such low MAX percentages are not alarming given the number and detail of classes and the level of compositional heterogeneity of the forest. It is clear that many of the more common errors within the map are due to intuitively obvious and generally acceptable mistakes that stem from the spectral overlap that exists among compositionally similar forest classes (Treitz *et al.*, 1992; Manyara and Lein, 1994). Overlays of our classified forest-type map with ancillary data sets (soils, elevation, slope, aspect)

TABLE 4. FUZZY ACCURACY ASSESSMENT–MAX-RIGHT CLASSIFICATION RESULTS. MEAN MAX PERCENTAGE IS 13.35, MEAN RIGHT PERCENTAGE IS 78.88

Class No.	Forest Type	# Sites	MAX Number	MAX Percent	RIGHT Number	RIGHT Percent	Increase Number	Increase Percent
1	*RO*	14	3	21.43	13	92.9	10	71.4
2	*RO/LU*	18	1	5.56	17	94.4	16	88.9
3	*RO/Mx*	12	0	0	8	66.7	8	66.7
4	*RO/MX/HU*	6	0	0	5	83.3	5	83.3
5	*RO/MX/LU*	10	0	0	6	60.0	6	60.0
6	*OAK/Mx*	6	0	0	3	50.0	3	50.0
7	*OAK/Mx/LU*	10	0	0	10	100.0	10	100.0
8	*RO/RM*	11	1	9.09	10	90.9	9	81.8
9	*RO/RM/LU*	8	0	0	8	100.0	8	100.0
10	*RO/RM/HU*	15	0	0	14	93.3	14	93.3
11	*RM*	3	0	0	2	66.7	2	66.7
12	*RM/HU*	5	1	20	5	100.0	4	80.0
13	*RM/LU*	3	0	0	2	66.7	2	66.7
14	*SM*	11	1	9.09	9	81.8	8	72.7
15	*SM/HU*	4	0	0	4	100.0	4	100.0
16	*SM/RO/Mx*	7	0	0	4	57.1	4	57.1
17	*WA/RM/Mx*	10	0	0	7	70.0	7	70.0
18	*WA/RM/Mx/PU*	6	1	16.67	4	66.7	3	50.0
19	*BC/SM/Mx*	1	1	100	1	100.0	0	0.0
20	*Be*	16	1	6.25	11	68.8	10	62.5
21	*Be/HU*	9	2	22.22	9	100.0	7	77.8
22	*NHd/Be/SM*	6	2	33.33	6	100.0	4	66.7
23	*NHd/Be/SM/HU*	13	0	0	10	76.9	10	76.9
24	*Hd/YB/RM/He*	8	0	0	5	62.5	5	62.5
25	*MxHd*	12	2	16.67	10	83.3	8	66.7
26	*MxHd/HU*	4	0	0	1	25.0	1	25.0
27	*Mx/Hd/WP*	12	1	8.33	9	75.0	8	66.7
28	*WP*	17	9	52.94	11	64.7	2	11.8
29	*P/MxConif*	3	1	33.33	3	100.0	2	66.7
30	*He/RM*	10	0	0	10	100.0	10	100.0
31	*He/MxHd*	21	2	9.52	17	81.0	15	71.4
32	*He*	28	12	42.86	19	67.9	7	25.0
33	*Sp*	3	1	33.33	1	33.3	0	0.0
	Mean			13.35%		78.88%		

validated both generalized species distribution patterns we observed in the field and matched patterns output from SORTIE (Kobe, 1996; Mickelson, 1997). For instance, our red maple classes occurred more frequently on wet soils and our oak classes dominated higher elevations and steeper terrain, matching commonly described species distributions (Egler, 1940; Winer, 1955; Damman, 1977; Kobe, 1996). Because this study focused on forest-type discrimination, we omitted non-forest classes from the accuracy assessment.

There are several reasons immediately apparent that would account for many of the classification errors. The large number of classes, the level of compositional and spectral similarity among classes, and the possible need for a more representative and better distributed training set are among the obvious (Wang, 1992). Additionally, while inter-image registration was found to approach the 0.5-pixel (15 metre) RMS error as stated by EOSAT, such a shift applied across three images with such a diverse forested land-cover pattern could in itself create a large degree of per-pixel spectral ambiguity. In addition, it should be noted that, because the majority of sample plots were specifically selected to avoid the boundary between forest types, the final classification may not adequately represent "edge classes." A change class was not incorporated within the classification, which, given the four-year interval between the spring and fall images, could ideally have accounted for harvested or burned forest cover as well as regenerated shrub areas.

Much of the output classification's value and limitations are apparent within the Fuzzy Accuracy Assessment CONFUSION and AMBIGUITY tables. While it is beyond the scope of this paper to discuss the detailed interactions among the 33 forest classes, we present CONFUSION and AMBIGUITY tables for the three broad dominant forest cover type groups found within the study area. These groups include the oaks (red, white, other), the maples (red, sugar), and the conifers (hemlock and pine). Combined, they account for more than two-thirds of the forest cover for the study site (Dickson and McAfee, 1988), and compositionally, they compose a similar percentage, 67 percent, of our 405 sample plots.

Tables 6 through 8 show pair-wise comparisons of three sets of commonly mistaken classes, red oak (*RO*) and red oak/mountain laurel (*RO/LU*) (6A and 6B), red maple (*RM*) and sugar maple (*SM*) (7A and 7B), and white pine (*WP*) and hemlock (*He*) (8A and 8B). The tables were constructed by sorting the combined omission errors found for each pair of classes, and show, in descending order, those forest types that were most commonly included within the two example classes. Significant composition overlap is apparent within the tables, which contain examples of the fuzzy CONFUSION and AMBIGUITY operator values. For instance, in Table 6A, the classes most commonly *confused*, or ranked higher in the classification than *RO* or *RO/LU*, possess a large oak component. The upper ten classes, which account for 74 percent of the combined sorted ommission errors, have a mean oak composition of 59 percent, compared to 14 percent for the remaining classes. The upper five classes exhibit an even more concentrated oak component, a mean of 79 percent, as compared to 19 percent for the remaining classes, and account for 50 percent of the combined omission errors. Clearly, oaks are mostly being confused with other oaks.

Table 6B lists the classes whose AMBIGUITY ranking equaled that of the *RO* or *RO/LU* class. There is nearly a two-thirds increase in the number of omission errors. However, an examination of the species compositions reveals that most of

Table 5. Fuzzy Accuracy Assessment–DIFFERENCE Table. Optimum DIFFERENCE Value Occurs when MAX Class Value Is 5 (Best Possible) Answer and all Others Are 1 (Completely Wrong), Yielding a DIFFERENCE of 4.

Class No.	Forest Type	N	−4	−3	−2	−1	1	2	3	4
1	*RO*	14	0	1	6	4	3	0	0	0
2	*RO/LU*	18	0	1	12	4	1	0	0	0
3	*RO/Mx*	12	2	2	4	4	0	0	0	0
4	*RO/MX/HU*	6	0	1	5	0	0	0	0	0
5	*RO/MX/LU*	10	0	4	4	2	0	0	0	0
6	*OAK/Mx*	6	1	2	1	2	0	0	0	0
7	*OAK/Mx/LU*	10	0	0	7	3	0	0	0	0
8	*RO/RM*	11	0	1	6	3	1	0	0	0
9	*RO/RM/LU*	8	0	0	8	0	0	0	0	0
10	*RO/RM/HU*	15	0	1	9	5	0	0	0	0
11	*RM*	3	0	1	2	0	0	0	0	0
12	*RM/HU*	5	0	0	4	0	1	0	0	0
13	*RM/LU*	3	0	1	2	0	0	0	0	0
14	*SM*	11	0	2	7	1	1	0	0	0
15	*SM/HU*	4	0	0	3	1	0	0	0	0
16	*SM/RO/Mx*	7	1	2	4	0	0	0	0	0
17	*WA/RM/Mx*	10	0	3	7	0	0	0	0	0
18	*WA/RM/Mx/PU*	6	1	1	3	0	0	1	0	0
19	*BC/SM/Mx*	1	0	0	0	0	0	1	0	0
20	*Be*	16	1	4	1	9	1	0	0	0
21	*Be/HU*	9	0	0	3	4	2	0	0	0
22	*NHd/Be/SM*	6	0	0	4	0	2	0	0	0
23	*NHd/Be/SM/HU*	13	1	2	10	0	0	0	0	0
24	*NHd/YB/RM/He*	8	1	2	5	0	0	0	0	0
25	*MxHd*	12	0	2	8	0	2	0	0	0
26	*MxHd/HU*	4	0	3	1	0	0	0	0	0
27	*Mx/Hd/WP*	12	1	2	7	1	0	1	0	0
28	*WP*	17	1	5	2	0	0	9	0	0
29	*P/MxConif*	3	0	0	2	0	0	1	0	0
30	*He/RM*	10	0	0	10	0	0	0	0	0
31	*He/MxHd*	21	1	3	15	0	0	2	0	0
32	*He*	28	0	9	4	3	12	0	0	0
33	*Sp*	3	0	2	0	0	0	0	1	0
	Total Plots	322								
	Percent	—	3.4%	17.7%	51.5%	14.2%	8.0%	4.6%	0.3%	0%

the errors can be understood and are *Acceptable*. The species overlap patterns are very similar to those found within the CONFUSION table. The upper ten classes account for 71 percent of the combined omission error, and have a mean oak percent of 54 percent, compared to 16 percent for the remaining classes.

The conifer-dominated classes at the bottom of the oak and maple CONFUSION and AMBIGUITY tables contain no commission errors, indicating a good measure of the separability between the oak/maple classes and the conifer groups. The strength of the species spectral response patterns can be considered to be the classification signal allowing for successful class separation. Conversely, the sum of the unaccounted variables (e.g., topographic effects, canopy crown density, intra-class and interdata spectral variability) (Bartlett *et al.*, 1988; Kharuk *et al.*, 1992), combined with the compositional and spectral ambiguity due to inter-class heterogeneity, can be considered to be classification noise. Below an undetermined signal threshold, which allows for the successful separation of the classes at the top and bottom of the tables, the classes within the middle of the tables likely have low signal-to-noise ratios. The errors found within these classes are more difficult to interpret in all our tables, and likely represent actual classification process error.

Within the *RM* and *SM* tables, similar CONFUSION and AMBIGUITY patterns are found although, compared to oak, the maple composition is less concentrated in the upper classes; the overall maple signal appears to be less strong. Both maple species were considered interchangeable within the accuracy assessment, and their percentage values in the CONFUSION and AMBIGUITY tables are considered as a combined group. Within the CONFUSION table (7A), the upper ten classes contain 61 percent of the combined ommission errors for *RM* and *SM*, but contain a mean of only 33 percent combined red maple or sugar maple versus 21 percent for the remaining classes. This difference is just significant, while the composition differences within all other tables are very significant at the 0.95 percent confidence level. The composition values increase slightly within the AMBIGUITY error table (Table 7B), with a mean combined maple percent of 40 percent for the upper ten classes and 18 percent for those remaining. While not all classes with high maple percentages are being included within the higher commission levels, the significant amount of maple that is within the upper classes likely contributes greatly to both the CONFUSION and AMBIGUITY errors.

The errors found within the *WP* and *He* classes (Tables 8A and 8B) follow patterns which are similar to those for oak and maple though their interpretation involves a bit more consideration. Genus level discrimination was accepted among oaks and maples while we ranked errors between white pine and hemlock as a fuzzy value of 2, meaning "understandable but wrong." All of the upper ten classes within both the CONFUSION and AMBIGUITY tables for *WP* and *He* contain a major coniferous component, 47 percent and 19 percent, respectively, within either the canopy or the sub-canopy. More specifically, where conifer errors occur, white pine and hemlock are typically being misclassified as each other. For example, within the CONFUSION table (Table 8A), looking at *He*, more than 80 percent of the upper ten CONFUSION errors have white pine as dominant or co-dominant (the mean *WP* percentage is

TABLE 6. FUZZY ACCURACY ASSESSMENT-RED OAK/RED OAK-LAUREL *CONFUSION* AND *AMBIGUITY* CLASS COMPARISONS. TABLE 6*A*. *CONFUSION*. BOLD LINE INDICATES UPPER TEN CLASSES, WHICH COLLECTIVELY ACCOUNT FOR 74 PERCENT OF THE COMBINED TOTAL OMISSION ERRORS FOR THE TWO CLASSES. MEAN OAK COMPOSITION FOR THESE TEN CLASSES IS 59 PERCENT, COMPARED TO 14 PERCENT FOR THE REMAINING CLASS. TABLE 6*B*. *AMBIGUITY*. BOLD LINE INDICATES UPPER TEN CLASSES, WHICH COLLECTIVELY ACCOUNT FOR 71 PERCENT OF THE COMBINED TOTAL OMISSION ERRORS FOR THE TWO CLASSES. MEAN OAK COMPOSITION FOR THESE TEN CLASSES IS 54 PERCENT COMPARED TO 16 PERCENT FOR THE REMAINING CLASSES.

Table 6A					Table 6B				
Class No.	Oak/Laurel Confusion: Class Name	RO	RO/LU	Total Omission	Class No.	Oak/Laurel Ambiguity: Class Name	RO	RO/LU	Total Omission
6	*OAK/Mx*	3	12	15	4	*RO/MX/HU*	5	11	16
3	*RO/Mx*	3	10	13	16	*SM/RO/Mx*	4	11	15
1	*RO*	X	10	10	5	*RO/MX/LU*	3	11	14
7	*OAK/Mx/LU*	2	4	6	8	*RO/RM*	3	11	14
10	*RO/RM/LU*	5	1	6	10	*RO/RM/LU*	1	12	13
8	*RO/RM*	4	2	6	9	*RO/RM/HU*	6	6	12
11	*RM*	4	2	6	7	*OAK/Mx/LU*	3	9	12
16	*SM/RO/Mx*	3	2	5	25	*MxHd*	5	6	11
5	*RO/MX/LU*	2	2	4	26	*MxHd/HU*	5	6	11
26	*RO/RM/HU*	2	1	3	6	*OAK/Mx*	7	2	9
25	*MxHd*	2	1	3	3	*RO/Mx*	6	3	9
14	*SM*	2	1	3	17	*RO/RM/LU*	4	2	6
12	*RM/HU*	2	1	3	2	*RO/LU*	5	X	5
13	*RM/LU*	2	1	3	1	*RO*	X	4	4
17	*WA/RM/Mx*	1	1	2	12	*RM/HU*	2	1	3
22	*NHd/Be/SM*	1	1	2	13	*RM/LU*	2	1	3
15	*SM/HU*	1	1	2	14	*SM*	2	1	3
9	*RO/RM/HU*	1	1	2	22	*NHd/Be/SM*	2	1	3
2	*RO/LU*	2	X	2	31	*He/MxHd*	1	1	2
23	*NHd/Be/RM/HU*	1	0	1	11	*RM*	1	1	2
19	*BC/SM/Mx*	0	1	1	23	*NHd/Be/RM/HU*	1	1	2
24	*NHd/YB/RM/He*	1	0	1	24	*NHd/YB/RM/He*	1	1	2
31	*He/MxHd*	1	0	1	27	*Mx/Hd/WP*	1	1	2
30	*He/RM*	0	0	0	15	*SM/HU*	1	0	1
21	*Be/HU*	0	0	0	30	*He/RM*	1	0	1
32	*He*	0	0	0	20	*Be*	0	1	1
20	*Be*	0	0	0	21	*Be/HU*	1	0	1
18	*WA/RM/WP/Mx*	0	0	0	19	*BC/SM/Mx*	1	0	1
27	*Mx/Hd/WP*	0	0	0	18	*WA/RM/WP/Mx*	0	1	1
4	*RO/MX/HU*	0	0	0	32	*He*	0	0	0
28	*WP*	0	0	0	33	*Sp*	0	0	0
29	*P/MxConif*	0	0	0	28	*WP*	0	0	0
33	*Sp*	0	0	0	29	*P/MxConif*	0	0	0
	Total commission	45	55	100		Total commission	74	105	179

26 percent for all ten classes, compared to 8 percent for the remaining classes). Conversely, classes which are erroneously being confused with *WP* contain a significant *He* composition, commonly in the sub-canopy (the mean *He* canopy composition for the upper ten classes is 21 percent versus 9 percent for the remaining classes, while the *HU* value is 7 for these classes compared to 3 for those remaining). The errors found within the AMBIGUITY table (Table 8B) are more diffuse, but more acceptable. As a group, the total conifer canopy composition is relatively low for the upper ten classes, 19 percent (7 percent *WP* and 12 percent *He*), though individually we find that seven out of the ten classes have a significant *He* component. Given the abundance of hemlock across the landscape, especially within mixed broadleaf-coniferous classes, such errors are understandable and even expected.

Our initial assumptions, matching the conclusions of Treitz (1992), that classes which were simpler (made up of one or two dominant species) tend to be easier to classify accurately, proved incorrect. A simple sorting of classes by number of significant canopy components, from greatest to fewest, showed no clear or coherent trend in terms of those classes which consistently scored higher and those which attained poor accuracy. In our study, class composition and heterogeneity seemed to have less effect on classification accuracy performance than did the sum of the unaccounted variables (Beaubien, 1979). Among the more consistent classes, pine and hemlock exhibited interesting patterns. They each had among the highest MAX classification accuracy, but among the lowest RIGHT; they improved little by applying the RIGHT metric, which is a somewhat relaxed level of acceptance. This means that the classes that were right were very right, but that the errors were more extreme, and class accuracy improved little by allowing for compositional flexibility or canopy-understory confusion among conifers. Among the single-species conifer classes, the white pine class more commonly included hemlock (commission error) than the hemlock class included white pine. The white-pine-dominated class had more commission than omission errors and so tends to be somewhat over-represented within the map. Comparisons with the USFS statistics for Litchfield county (Dickson and McAfee, 1988) confirm this pattern, with their estimates for hemlock accounting for nearly two to three times the areal extent of white pine. Knowledge of this sort is useful when considering methods for improving map accuracy, especially when delineating classes with overlapping composition.

The most common DIFFERENCE value returned in our analysis, that of −2 (Table 9), accounted for a total of 51.5 percent of all sample plots and cumulatively 78.5 percent of all of our test plots were ranked at or above this value. This suggests that the detail of the classes may be in excess of what can be reasonably and successfully resolved at the species level, using this method. However, review of the expert evaluation de-

TABLE 7. RED MAPLE/SUGAR MAPLE *CONFUSION* AND *AMBIGUITY* CLASS COMPARISON. TABLE 7*A*. *CONFUSION*. BOLD LINE INDICATES UPPER TEN CLASSES, WHICH COLLECTIVELY ACCOUNT FOR 61 PERCENT OF THE COMBINED TOTAL OMISSION ERRORS FOR THE TWO CLASSES. MEAN COMBINED MAPLE COMPOSITION FOR THESE TEN CLASSES IS 33 PERCENT, COMPARED TO 21 PERCENT FOR THE REMAINING CLASSES. TABLE 7*B*. *AMBIGUITY*. BOLD LINE INDICATES UPPER TEN CLASSES, WHICH COLLECTIVELY ACCOUNT FOR 58 PERCENT OF THE COMBINED TOTAL OMISSION ERRORS FOR THE TWO CLASSES. MEAN COMBINED MAPLE COMPOSITION FOR THESE TEN CLASSES IS 40 PERCENT COMPARED TO 18 PERCENT FOR THE REMAINING CLASSES.

Table 7A					Table 7B				
Class No.	RM/SM Confusion			Total Omission	Class No.	RM/SM Ambiguity			Total Omission
	Class Name	RM	SM			Class Name	RM	SM	
16	*SM/RO/Mx*	1	4	5	26	*MxHd/HU*	2	8	10
8	*RO/RM*	0	4	4	13	*RM/LU*	0	9	9
9	*RO/RM/HU*	0	4	4	17	*WA/RM/Mx*	0	9	9
19	*BC/SM/Mx*	1	3	4	22	*NHd/Be/SM*	2	7	9
17	*WA/RM/Mx*	3	0	3	25	*MxHd*	3	6	9
4	*RO/MX/HU*	0	2	2	12	*RM/HU*	0	8	8
12	*RM/HU*	1	1	2	15	*SM/HU*	2	6	8
15	*SM/HU*	1	1	2	10	*RO/RM/LU*	3	4	7
22	*NHd/Be/SM*	1	1	2	16	*SM/RO/Mx*	2	5	7
23	*NHd/Be/RM/HU*	0	2	2	11	*RM*	X	6	6
26	*MxHd/HU*	1	1	2	19	*BC/SM/Mx*	2	4	6
1	*RO*	0	1	1	5	*RO/MX/LU*	1	4	5
2	*RO/LU*	0	1	1	8	*RO/RM*	3	2	5
3	*RO/Mx*	0	1	1	2	*RO/LU*	0	4	4
5	*RO/MX/LU*	0	1	1	3	*RO/Mx*	0	4	4
6	*OAK/Mx*	0	1	1	7	*OAK/Mx/LU*	0	4	4
7	*OAK/Mx/LU*	0	1	1	9	*RO/RM/HU*	3	1	4
10	*RO/RM/LU*	0	1	1	27	*Mx/Hd/WP*	0	4	4
11	*RM*	X	1	1	1	*RO*	0	3	3
13	*RM/LU*	1	0	1	4	*RO/MX/HU*	0	3	3
14	*SM*	1	X	1	6	*OAK/Mx*	0	3	3
20	*Be*	0	1	1	18	*WA/RM/WP/Mx*	3	0	3
21	*Be/HU*	0	1	1	14	*SM*	2	X	2
24	*NHd/YB/RM/He*	0	1	1	24	*NHd/YB/RM/He*	1	1	2
27	*Mx/Hd/WP*	1	0	1	21	*Be/HU*	0	1	1
30	*He/RM*	0	1	1	23	*NHd/Be/RM/HU*	1	0	1
31	*He/MxHd*	0	1	1	28	*WP*	0	1	1
32	*He*	0	1	1	29	*P/MxConif*	0	1	1
18	*WA/RM/WP/Mx*	0	0	0	30	*He/RM*	0	1	1
25	*MxHd*	0	0	0	31	*He/MxHd*	1	0	1
28	*WP*	0	0	0	33	*Sp*	0	1	1
29	*P/MxConif*	0	0	0	20	*Be*	0	0	0
33	*Sp*	0	0	0	32	*He*	0	0	0
	Total commission	12	37	49		Total commission	31	110	141

cision tree shows that at the genus level, or the stage where a class was considered to be acceptable, the method works quite well, with an overall forest classification accuracy rivaling maps with far fewer and less detailed classes. The patterns displayed within the DIFFERENCE table also reinforce the broadness and frequency of class overlap.

Summary

The forest classification results provide encouraging support for the method. It is apparent that seasonal species-specific spectral signals, as represented within TM data, are strong enough to aid greatly in the mapping of the mixed deciduous forests of the northeastern United States. Utilizing the spectral patterns from within a combined spring/summer/fall image, we obtained satisfactory forest-type classification accuracy (78.9 percent) at the genus level, delineating a total of 33 forest-type classes, with thematic detail as fine as Anderson Level 4 for sub-categorical understory classes. Preliminary discriminant analysis between the three dates indicated that spring and fall data are potentially more useful than those acquired during summer, and it is likely that utilizing well-timed image acquisition dates from within these periods, combined with specific knowledge of canopy and understory phenologies, can improve discrimination further. For detailed vegetation mapping, the GPS is clearly valuable for referencing the spectral patterns found within multi-date imagery to the specific vegetation composition of individual forest stands.

The forest-type classification we adopted was tailored towards our own research needs, though such an approach has broad utilization for regional biodiversity and vegetation mapping, forest inventorying and ecological analysis for the forests of the Northeast. Seasonally acquired satellite data could supply the foundation for a hybrid vegetation classification system which could deliver map units approaching the Federal Geographic Data Committee's (FGDC) *community* and *alliance* level (USGS, 1996). This would greatly aid the efforts of such programs as the National GAP Analysis project (Scott *et al.*, 1993) and others needing detailed vegetative land-cover information.

While it seems unlikely that vegetation cover types for the forests of the Northeast can be delineated consistently at the FGDC *community* or *alliance* level (USGS/NGDC, 1996) when using strictly spectral information and computer-derived classifications, much work needs to be undertaken to evaluate the maximum level of vegetation information contained within satellite-derived remotely sensed data. A wide variety of techniques and methodologies are currently being employed to improve delineation of the forests of this region, and it is likely that an optimum strategy would make use of aspects of each. Adding derived information (band ratios, veg-

Table 8. White Pine/Hemlock *Confusion* and *Ambiguity* Class Comparison. Table 8*A*. *Confusion*. Bold Line Indicates Upper Ten Classes, Which Collectively Account for 58 Percent of the Combined Total Omission Errors for the Two Classes. Mean White Pine Composition for These Ten Classes is 26 Percent Compared to 8 Percent for the Remaining Classes. Mean Hemlock Canopy Composition for This Group Is 21 Percent Versus 9 for the Remaining Classes. Mean Hemlock Understory Value is 7 Versus 3 for the Remaining Classes. Total Conifer Composition Is 47 Percent for the Canopy with a Significant Hemlock Understory Component. Table 8*B*. *Ambiguity*. Bold Line Indicates Upper Ten Classes, Which Collectively Account for 67 Percent of the Combined Total Omission Errors for the Two Classes. Mean White Pine Composition for These Ten Classes Is 7 Percent, Compared to 10 Percent for the Remaining Classes. Mean Hemlock Canopy Composition for This Group Is 8 Percent Versus 8 Percent for the Remaining Classes. Mean Hemlock Understory Value Is 8 Versus 3 for the Remaining Classes.

Table 8A					Table 8B				
Class No.	WP/TC Confusion Class Name	WP	He	Total Omission	Class No.	WP/TC Ambiguity Class Name	WP	He	Total Omission
27	*Mx/Hd/WP*	2	8	10	30	*He/RM*	1	13	14
29	*P/MxConif*	1	8	9	12	*RM/HU*	2	12	14
28	*WP*	X	8	8	23	*NHd/Be/RM/HU*	2	12	14
30	*He/RM*	5	3	8	24	*NHd/YB/RM/He*	2	12	14
31	*He/MxHd*	3	4	7	33	*Sp*	3	7	10
18	*WA/RM/WP/Mx*	0	7	7	26	*MxHd/HU*	1	8	9
4	*RO/MX/HU*	5	0	5	9	*RO/RM/HU*	0	8	8
9	*RO/RM/HU*	5	0	5	11	*RM*	4	4	8
26	*MxHd/HU*	5	0	5	15	*SM/HU*	2	5	7
32	*He*	3	X	3	18	*WA/RM/WP/Mx*	5	2	7
15	*SM/HU*	3	0	3	31	*He/MxHd*	3	2	5
8	*RO/RM*	3	0	3	27	*Mx/Hd/WP*	5	0	5
10	*RO/RM/LU*	3	0	3	29	*P/MxConif*	4	0	4
12	*RM/HU*	3	0	3	17	*WA/RM/Mx*	4	0	4
16	*SM/RO/Mx*	3	0	3	22	*NHd/Be/SM*	4	0	4
1	*RO/RM/HU*	3	0	3	25	*MxHd*	4	0	4
5	*RO/MX/LU*	3	0	3	2	*RO/LU*	3	0	3
21	*Be/HU*	3	0	3	3	*RO/Mx*	3	0	3
23	*NHd/Be/RM/HU*	3	0	3	7	*OAK/Mx/LU*	3	0	3
24	*NHd/YB/RM/He*	3	0	3	32	*He*	3	X	3
33	*Sp*	1	1	2	5	*RO/MX/LU*	2	0	2
2	*RO/LU*	2	0	2	8	*RO/RM*	2	0	2
3	*RO/Mx*	2	0	2	10	*RO/RM/LU*	2	0	2
6	*OAK/Mx*	2	0	2	13	*RM/LU*	2	0	2
7	*OAK/Mx/LU*	2	0	2	16	*SM/RO/Mx*	2	0	2
11	*RM*	1	0	1	21	*Be/HU*	2	0	2
14	*SM*	1	0	1	6	*OAK/Mx*	1	0	1
13	*RM/LU*	1	0	1	19	*BC/SM/Mx*	1	0	1
17	*WA/RM/Mx*	1	0	1	28	*WP*	X	1	1
19	*BC/SM/Mx*	1	0	1	1	*RO*	0	0	0
20	*Be*	1	0	1	4	*RO/MX/HU*	0	0	0
22	*NHd/Be/SM*	1	0	1	14	*SM*	0	0	0
25	*MxHd*	1	0	1	20	*Be*	0	0	0
	Total commission	76	39	115		Total commission	72	86	158

etation indices, or texture indices), physical data (soil moisture, slope, aspect, elevation), structural stand information (canopy height, percent cover, understory composition and density), as well as site specific vegetation knowledge (phenology), would likely improve the thematic map resolution of these forests. Improved processes and algorithms such as subpixel classifiers, resolution merging enhancements, and neural network classifiers might contribute to the more detailed pattern extraction capabilities that will be needed.

Table 9. Fuzzy Accuracy Assessment-Percent and Cumulative Percent Class DIFFERENCE Totals

Difference Value	% of SP/Value	Total Cumulative %
4	0.00%	0.00%
3	0.31%	0.31%
2	4.66%	4.97%
1	8.07%	13.01%
−1	14.29%	27.30%
−2	51.55%	78.88%
−3	17.70%	96.58%
−4	3.42%	100%

Acknowledgments

We are indebted to the Edward Childs family, who generously allowed the use of Great Mountain Forest and its facilities as a base for our field data collection. We thank Jennifer Jenkins for her graciously sharing her GPS sample plot data. We gratefully acknowledge and appreciate the grant support of NSF (BSR-8918616, DEB-9221097, DEB-9220620), the United States Deptartment of Energy (DE-FG02-90ER60933 and DE-FG02-94ER1815), and NASA (NAGW-2088, NAGW-3471, NAGW-3703).

References

Anderson, J.R., E.E. Hardy, J.T. Roach, and R.E Witmer, 1976. *A Land Use Land Cover Classification System for Use with Remote Sensor Data*, Geological Survey Professional Paper-964, USGS, Washington, D.C.

Banyikawa, F.F., E. Feoli, and V. Zuccarello, 1990. Fuzzy set ordination and classification of Serengeti short grasslands, Tanzania, *Journal of Veg. Science*, 1:97–104.

Bartlett, D.S., M.A. Hardisky, R.W. Johnson, M.G. Gross, V. Klemass, and J.M. Hartman, 1988. Continental scale variability in vegetation reflectance and its relationship to canopy morphology, *Int. Journal of Remote Sensing*, 9(7):1223–1241.

Bauer, M.E., T.E. Burk, A.R. Ek, P.R. Coppin, S.D. Lime, T.A Walsh, D.K. Walters, W. Befort, and D.F. Heinzen, 1994. Satellite inventory of Minnesota forest resources, *Photogrammetric Engineering & Remote Sensing*, 60(3):287–298.

Beaubien, Jean, 1979. Forest type mapping from Landsat digital data, *Photogrammetric Engineering & Remote Sensing*, 45(8):1135–1144.

Benson, A., and S.D. DeGloria, 1985. Interpretation of Landsat–4 Thematic Mapper and Multispectral Scanner data for forest surveys, *Photogrammetric Engineering & Remote Sensing*, 51(9):1281–1289.

Bolstad, P.V., and T.M. Lillesand, 1992. Improved classification of forest vegetation in Northern Wisconsin through a rule-based combination of soils, terrain, and Landsat Thematic Mapper data, *Forest Science*, 38(1):5–20.

Brown, J.F., T.R. Loveland, J.W. Merchant, B.C. Reed, and D.O. Ohlen, 1993. Using multisource data in global land-cover characterization: Concepts, requirements, and methods, *Photogrammetric Engineering & Remote Sensing*, 59(6):977–987.

Bryant, E., A.G. Dodge, and S.D. Warren, 1980. Landsat for practical forest type mapping: A test case, *Photogrammetric Engineering & Remote Sensing*, 46(12):1575–1584.

Congalton, R.G., 1991. A review of assessing the accuracy of classifications of remotely sensed data, *Remote Sensing of Environment*, 37:35–46.

Collins, J.D., 1994. *Fuzzy Accuracy Assessment Software Program*, Department of Geography, Boston University, Boston, Massachusetts.

Curran, P.J., J.L. Dungan, B.A. Macler, and S.E. Plummer, 1991. The effect of a red leaf pigment on the relationship between red edge and chlorophyll concentration, *Remote Sensing of Environment*, 35:69–76.

Damman, A.W.H., 1979. The role of vegetation pattern change analysis in land classification, *The Forestry Chronicle*, 55(5):175–182.

Damman, A.W.H., and B. Kershner, 1977. Floristic composition and topographical distribution of the forest communities of the gneiss areas of western Connecticut, *Le Naturaliste Canadien*, 104:23–45.

Dickson, D.R., and C.R. McAfee, 1988. *Forest Statistics for Connecticut–1972-1985*, Resource Bulletin-NE-105, USDA Forest Service, Broomall, Pennsylvania.

Egler, Frank E., 1940. Berkshire Plateau Vegetation, Massachusetts, *Ecological Monographs*, 10(2):147–192.

Eyre, F.H., 1980. *Forest Cover Types of the United States and Canada*, The Society of American Foresters, Washington, D.C.

Fernald, M.L., 1988. *Gray's Manual of Botany: A Handbook of the Flowering Plants and Ferns of the Central and Northeastern United States and Canada*, Dioscorides Press, Portland, Oregon.

Foster, D.R., 1992. Land-use dynamics (1730–1990) and vegetation dynamics in central New England, USA, *Journal of Ecology*, 80:753–772.

———, 1993. Land-use history and forest transformations in central New England, *Humans as Components of Ecosystems* (M. McDonnell, editor), Springer–Verlag, New York, pp. 91–110.

Franklin, J., T.L. Logan, C.E. Woodcock, and A.H. Strahler, 1986. Coniferous forest classification and inventory using Landsat and digital terrain data, *IEEE Transactions on Geoscience and Remote Sensing*, 24:139–149.

Franklin, S.E., and D.R. Peddle, 1989. Spectral texture for improved class discrimination in complex terrain, *Int. Journal of Remote Sensing*, 10(8):1437–1443.

Goodchild, Michael F., 1994. Integrating GIS and remote sensing for vegetation analysis and modeling: Methodological issues, *Journal of Vegetation Science*, 5:615–626.

Gopal, S., and C. Woodcock, 1994. Theory and methods for accuracy assessment of thematic maps using fuzzy sets, *Photogrammetric Engineering & Remote Sensing*, 60(2):181–188.

Goward, S.N., J.T. Compton, and D.G. Dye, 1985. North American vegetation patterns observed with the NOAA-7 Advanced Very High Resolution Radiometer, *Vegetatio*, 64:3–14.

Herwitz, S.R., D.L. Peterson, and J.R. Eastman, 1990. Thematic Mapper detection of changes in the leaf area of closed canopy pine plantations in Central Massachusetts, *Remote Sensing of Environment*, 29:129–140.

Hixon, M., D. Scholz, N. Fuhs, and T. Akiyama, 1980. Evaluation of several schemes for classification of remotely sensed data, *Photogrammetric Engineering & Remote Sensing*, 46(12):1547–1553.

Karteris, Michael A., 1990. The utility of digital Thematic Mapper data for natural resource classification, *Int. Journal of Remote Sensing*, 11(9):1589–1598.

Kharuk, V.I., A.M. Alshansky, and V.V. Yegorov, 1992. Spectral characteristics of vegetation cover: Factors of variability, *Int. Journal of Remote Sensing*, 13(17):3263–3272.

Kobe, R.K., S.W. Pacala, J.A. Silander, Jr., and C.D. Canham, 1995. Juvenile tree survivorship as a component of shade tolerance, *Ecological Applications*, 5:517–532.

Kobe, R.K., J.A. Silander, Jr., and J.G. Mickelson, Jr., 1996. Forest community structure and dynamics in northeastern North America: scaling from the individual to the landscape, *Journal of Vegetation Science* (in review).

Lee, K.S., W.D. Philpot, and S.W. Pacala, 1992. Calibration of a forest ecosystem model using remote sensing and GIS, *Proceedings, ASPRS/ACSM/RT 92', Monitoring and Mapping Global Change*, ASPRS/ACSM, Washington, D.C., 4:20–29.

Loveland, T.R., J.W. Merchant, and D.O. Ohlen, 1991. Development of a land-cover characteristics databaase for the conterminous U.S., *Photogrammetric Engineering & Remote Sensing*, 57(11):1453–1463.

Ludwig, J.A., and J.F. Reynolds, 1988. *Statistical Ecology: A Primer of Methods and Computing*, John Wiley and Sons, New York, 337 p.

Manyara, C.G., and J.K. Lein, 1994. Exploring the suitability of fuzzy set theory in image classification: A comparative study applied to the Mau Forest Area Kenya, *Proceedings, 1994 ASPRS/ACSM Annual Convention & Exposition*, Reno, Nevada, ASPRS, pp. 384–391.

Moore, M.M., and M.E. Bauer, 1990. Classification of forest vegetation in North-Central Minnesota using Landsat Multispectral Scanner adn Thematic Mapper Data, *Forest Science*, 36(2):330–342.

Nelson, R.F., R.S. Latty, and G. Mott, 1984. Classifying northern forests using Thematic Mapper Simulator data, *Photogrammetric Engineering & Remote Sensing*, 50(5): 607–617.

Pacala, S.W., C.D. Canham, and J.A. Silander, Jr., 1993. Forest models defined by field measurements: I. The design of a northeastern forest simulator, *Canadian Journal of Forest Research*, 23:1980–1988.

Pacala, S.W., C.D. Canham, J.A. Silander, and R.K. Kobe., 1996. Forest models defined by field measurements: 2. Estimation, error, analysis, and dynamics, *Ecological Monographs* (in press).

Reed, Bradley C., J.F. Brown, D. VanderZee, T.R. Loveland, J.W. Merchant, and D.O. Ohlen, 1994. Measuring phenological variability from satellite imagery, *Journal of Vegetation Science*, 5:703–714.

Richards, J.A., 1986. *Remote Sensing Digital Image Analysis: An Introduction*, Springer–Verlag, New York.

Ripple, W.J., 1986. Spectral reflectance relationships to leaf water stress, *Photogrammetric Engineering & Remote Sensing*, 10:1669–1675.

Rock, B.R., and J.E. Vogelmann, 1989. Use of Thematic Mapper Data for the detection of forest damage caused by the pear thrips, *Remote Sensing of Environment*, 30:217–225.

Schriever, J., and R.G. Congalton, 1995. Evaluating seasonal variability as an aid to cover-type mapping from Landsat Thematic Mapper data in the Northeast, *Photogrammetric Engineering & Remote Sensing*, 61(3):321–327.

Slaymaker, Dana M., K.M.L. Jones, C.R. Griffin, and J.T. Finn, 1995. Mapping deciduous forests in New England using aerial videography and multi-temporal Landsat TM imagery, *Proceedings, GAP Analysis Symposium*, Charlotte, North Carolina, ASPRS.

Smith, Don, 1992. *Weekly Fall Foliage Report, Fall Foliage Report*, State of Connecticut DEP Bureau of Natural Resources – Forestry Division.

Spanner, M.A., L.L. Pierce, D.L. Peterson, and S.W. Running, 1990. Remote sensing of temperate coniferous forest leaf area index: The influence of canopy closure, understory vegetation and background reflectance, *Int. Journal of Remote Sensing*, 11(1):95–111.

Stenback, Janine M., and R.G. Congalton, 1990. Using Thematic Mapper imagery to examine forest understory, *Photogrammetric Engineering & Remote Sensing*, 56(9):1285–1290.

Thomasson, J.A., C.W. Bennett, B.D. Jackson, and M.P. Mailander, 1994. Differentiating bottomland tree species with multispectral videography, *Photogrammetric Engineering & Remote Sensing*, 60(1):55–59.

Thompson, B.C., P.J Crist, J.S. Prior-Magee, R.A. Deitner, D. Garber, and M.A. Hughes, 1996. *Gap Analysis of Biological Diversity Conservation in New Mexico Using Geographic Information Systems, Final Gap Analysis Report*, USDI, New Mexico Cooperative Fish and Wildlife Service Unit, Las Cruses, New Mexico.

Townshend, John, C. Justice, W. Li, C. Gurney, and J. McManus, 1991. Global land cover classification by remote sensing: Present capabilities and future possibilities, *Remote Sensing of the Environment*, 35:243–255.

Treitz, Paul M., P.J. Howarth, and R.C. Suffling, 1992. Application of detailed ground information to vegetation mapping with high spatial resolution digital imagery, *Remote Sensing of Environment*, 42:65–82.

Varjo, J., 1996. Controlling continuously updated forest data by satellite remote sensing, *Int. Journal of Remote Sensing*, 10(34):43–67.

Vogelmann, J.E., 1988. Detection of forest change in the Green Mountains of Vermont using Multispectral Scanner data, *Int. Journal of Remote Sensing*, 9(7):1187–1200.

Vogelmann, J.E., and B.N. Rock, 1986. Assessing forest decline in coniferous forests of Vermont using NS-001 Thematic Mapper simulator data, *Int. Journal of Remote Sensing*, 7(10):1303–1321.

———, 1989. Use of Thematic Mapper data for the detection of forest damage caused by the pear thrip, *Remote Sensing of Environment.*, 30:217–225.

Wang, Fangju, 1990. Improving remote sensing image analysis through fuzzy information representation, *Photogrammetric Engineering & Remote Sensing*, 56(8):1163–1169.

Wang, Yeqiao, 1992. *Spatial Modeling Augmented Classification of Satellite Derived Land Use and Land Cover Information*, Masters Thesis, University of Connecticut.

Wang, Y., and D.L. Civco, 1992. Post-classification of misclassified pixels by evidential reasoning: A GIS approach for improving classification accuracy of remote sensing data, *Proceedings, ASPRS/ACSM/RT'92*, Washington D.C., ASPRS, pp. 160–170.

Westveldt, M., R.I. Ashman, H.I. Baldwin, R.P. Holdsworth, R.S. Hobnson, J.H. Lambert, H.J. Lutz, L. Swain, and M. Standish, 1956. *Natural Forest Vegetation Zones of New England*, Society of American Foresters.

Winer, H.I., 1955. *History of the Great Mountain Forest, Litchfield County, Connecticut*, Doctoral Dissertation, Yale School of Forestry and Environmental Studies.

Wolter, Peter T., D.J. Mladenoff, G.E. Host G.E., and T.R. Crow, 1995. Improved forest classification in the northern lake states using multi-temporal Landsat imagery, *Photogrammetric Engineering & Remote Sensing*, 61(9):1129–1143.

Woodcock, C.E., and A.H. Strahler, 1987. The factor of scale in remote sensing, *Remote Sensing of Environment*, 21:211–332.

Woodcock, C., and S. Gopal, 1992. Accuracy assessment of the Stanislaus Forest vegetation map using fuzzy sets, *Proceedings of the Fourth Biennial Remote Sensing Applications Conference*, Orlando, Florida, USDA Forest Service, USDI Fish & Wildlife Service, 17 p.

Woodcock, C.E., J. Collins, S. Gopal, V. Jakabhazy, X. Li, S. Macomber, S. Ryherd, Y. Wu, V.J. Harward, J. Levitan, and R. Warbington, 1994. Mapping forest vegetation using Landsat TM imagery and a canopy reflectance model, *Remote Sensing of Environment*, 50(3):240–254.

Zadeh, L.A., 1965. Fuzzy sets, *Information and Control*, 8:338–353.

Zeff, I.S., and C.J.Merry, 1993. Thematic mapper data for forest resource allocation, *Photogrammetric Engineering & Remote Sensing*, 59(1):93–99.

Zhu, A., and D.L. Evans, 1994, U.S. forest types and predicted percent forest cover from AVHRR data, *Photogrammetric Engineering & Remote Sensing*, 60(5):525–531.

Zhu, Zhiliang, 1994. *Forest Density Mapping in the Lower 48 States: A Regression Procedure*, Research Paper-SO-280, USDA Forest Service, Southern Forest Experiment Station.

Zhuang, X., B.A. Engel, X. Xiong, and C.J. Johannsen, 1995. Analysis of classification results of remotely sensed data and evaluation of classification algorithms, *Photogrammetric Engineering & Remote Sensing*, 61(4):427–433.

(Received 20 March 1997; revised and accepted 23 January 1998; revised 13 February 1998)